Original article

STAT3-siRNA induced B16.F10 melanoma cell death: more association with VEGF downregulation than p-STAT3 knockdown

Aws Alshamsan *

Nanomedicine Research Unit, Department of Pharmaceutics, College of Pharmacy, King Saud University, Saudi Arabia
King Abdullah Institute for Nanotechnology, King Saud University, Saudi Arabia

ABSTRACT

STAT3 knockdown by small interfering RNA (siRNA) has been described to inhibit carcinogenic growth in various types of tumors. Earlier we have reported delivery of siRNA by oleic acid- and stearic acid-modified-polyethylenimine and enhancement of silencing of STAT3 by small interfering RNA (siRNA) in B16.F10 melanoma cell lines and consequent tumor suppression. Present investigation mainly focused on the downstream events involved in B16.F10 melanoma cell death and consequent tumor suppression following knockdown of p-STAT3 by siRNA. Lipid-substituted polyethylenimine (PEI)-p-STAT3-siRNA were prepared and characterized by measuring its N/P ratio, zeta potential, size, association and dissociation with siRNA. B16.F10 melanoma cells were treated with six different concentrations of PEI-p-STAT3-siRNA (200, 100, 50, 25, 12.5 and 6.25 nM). Downregulation of p-STAT3 and VEGF were studied using western blot and ELISA in association with the melanoma cell death. PEI-p-STAT3-siRNA hydrodynamic diameter ranged from 110 to 270 nm. PEI assisted p-STAT3-siRNA delivery exhibited increased uptake by B16.F10, when analyzed by fluorescent and confocal microscopy along with flowcytometry. It induced concentration-dependent knockdown of the p-STAT3 that also downregulated VEGF expression in similar fashion and induced B16.F10 cell death. Higher concentrations of p-STAT3-siRNA appear to significantly downregulate the VEGF expression via p-STAT3 knockdown. Decreasing survival of B16.F10 cells with the increasing concentration of p-STAT3-siRNA significantly correlated with VEGF downregulation, not with p-STAT3 expression. Data suggest that VEGF downregulation following knockdown of p-STAT3 may be a key event in survival reduction in B16.F10 melanoma cells and.

1. Introduction

Last decade of cancer investigations has witnessed the emergence of signal transducer and activator of transcription 3 (STAT3) as a target for cancer therapies (Yu et al., 2014; Johnson et al., 2018). STAT3, which is a transcription factor that regulates expression of genes associated with cell survival, cell cycle, and immune response linked to carcinogenic progression, has been proved to be a promising target for tumor suppression (Yue and Turkson, 2009; Dutta et al., 2014; Furtek et al., 2016). It is reported to be

aberrantly activated in around 70% cases of hematological and solid cancers (Dutta et al., 2014). STAT3 also plays a leading role in regulating immune responses in the tumor microenvironment and when obstinately activated it promotes tumor survival and proliferation via suppressing anti-tumor immune responses (Yu et al., 2009). Angiogenesis via vascular endothelial growth factor (VEGF) overexpression remains central to tumor proliferation as well as cancer treatment (Carmeliet, 2005; Kut et al., 2007) and STAT3 activation regulates the expression of VEGF. Constitutively activated STAT3 increases VEGF expression and promotes cancerous growth; this direct association of the STAT3 in tumor proliferation also makes it a suitable target for cancer treatment (Wei et al., 2003).

VEGF, which was identified as an endothelial mitogen, has potential to induce pathological angiogenesis, other than its normal functions. VEGF-mediated signaling, in tumors, plays a crucial role in cancer stem cell functions and tumor initiation (Goel and Mercurio, 2013). Other than its normal functions of angiogenesis and vascular permeability, VEGF also modulates immune

* Address: P.O. Box 2457, Riyadh 11451, Saudi Arabia.
E-mail address: aalshamsan@ksu.edu.sa
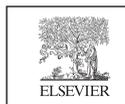
responses in the tumor microenvironment and affect host responses to tumors (Hansen et al., 2012). Targeting upstream to the VEGF, which is STAT3, can affect all the signaling activities downstream, either in normal or cancerous conditions.

Small interfering RNA (siRNA) mediated inhibitory effects, on specific genes and their products, is an emerging strategy in pharmacology and therapeutics. Specific gene products in form of mRNA are silenced siRNA, thus inhibiting protein translation. This specific inhibitory effect along with minimal chances of undesired effects and toxicities are among the advantages of siRNA over pharmaceutical agents of chemical origin. Specific siRNAs have been used to exhibit their inhibitory activities in breast and liver cancer cells *in-vitro* (Azimi et al., 2017; Huang et al., 2017). However, it appears to be marred by poor cellular uptake, short half-life, and unspecific distribution of siRNA into the body. Several approaches have been proposed to tackle these issues with using siRNAs as therapeutic agents. Nanomedicinal approaches appear to be promising in this regard. Recently several nanoformulation approaches have been proposed to improve the siRNA delivery and effects. PLGA encapsulating siRNA (De Rosa and Salzano, 2015), Calcium-siRNA nanocomplexes (Ruvinov et al., 2015), amphiphilic poly(α)glutamate polymeric micelles (Krivitsky et al., 2017) are few among such approaches.

In our earlier publications we have reported tumor suppressive activities of STAT3-siRNA in B16.F10 melanoma cells, which was enhanced by incorporation of oleic acid- and stearic acid-modified-polyethylenimine (PEI-STAT3-siRNA). This lipid-substituted polyethylenimine polymeric system was developed to assist the siRNA delivery and enhance the intracellular uptake (Alshamsan et al., 2009). This approach was found to improve the apoptotic effects of STAT3-siRNA in B16 melanoma cells *in-vitro* and suppressed tumors *in-vivo* in mice model (Alshamsan et al., 2010). It was also demonstrated that PEI-STAT3-siRNA also improved the immune responses against cancerous progression in B16.F10 melanoma both *in-vitro* and *in-vivo* (Alshamsan et al., 2011).

The present investigation is a continuation of the work from previous research reports (Alshamsan et al., 2010). Keeping in mind, the STAT3 aberrant functions and involvement of downstream VEGF in tumor angiogenesis, present investigation explored effects of PEI-STAT3-siRNA induced knockdown of the p-STAT3, VEGF expression, and suppression in B16.F10 melanoma cells. The study also focused on improving the formulation of PEI-STAT3-siRNA nanocomplexes and their uptake by, and overall effect on survival of B16.F10 melanoma cells.

2. Material

Branched PEI (25 kDa), glycerol, 3-(4,5-Dimethylthiazol-2-yl)-2,5-diphenyltetrazolium bromide (MTT), acrylamide/bis-acrylamide (19:1), dimethyl sulfoxide (DMSO), sodium orthovanadate (Na_3VO_4), ethylene glycol-bis(2-aminoethylether)-*N,N,N′,N′*-tetraacetic acid (EGTA), 2-mercaptoethanol, HEPES sodium salt, phosphate buffered saline (PBS) powder (pH 7.4), TWEEN® 20, paraformaldehyde, polyvinylidene difluoride (PVDF) membrane, sodium dodecyl sulfate (SDS), tris-HCl, Tris-Glycine SDS Running Buffer, and heparin were obtained from Sigma-Aldrich (St. Louis, MO). Fetal bovine serum (FBS), Dulbecco's Modified Eagle's Medium (DMEM), L-glutamine, gentamicin, 4′,6-diamidino-2-phenylindole (DAPI), Dextran-Texas Red™, mouse VEGF ELISA Kit, Sequence-specific siRNA targeting murine STAT3 mRNA (sense: 5′-GGACGACUUUGAUUUCAACtt-3′, anti-sense: 5′-GUUGAAAUCAAAGUCGUCCtg-3′), Silencer™ FAM-labeled Negative Control #1 siRNA (Catalogue #AM4620), dithiothreitol (DTT), Nonidet P40 (NP-40) detergent solution, protease/phosphatase inhibitor

cocktail, bromophenol blue, Bolt® Transfer Buffer, tetramethylethylethylenediamine (TEMED), Blocker™ BSA, ammonium persulfate (APS), and Micro BCA™ Protein Assay Kit were obtained from Thermo Fisher Scientific (Waltham, MA). Anti-phosphotyrosine (Y^{705}) STAT3 monoclonal antibody, and anti-actin antibody (I-19) were purchased from Santa Cruz Biotechnology (Stanta Cruz. CA). Amersham ECL Prime Western Blotting Detection Reagent kit was purchased from GE Healthcare Life Sciences (Piscataway, NJ). B16.F10 ATCC® CRL-6475™ was obtained from American Type Culture Collection (ATCC).

3. Methods

3.1. Preparation and characterization of siRNA polyplexes

In sterile Eppendorf tubes, PEI solution was added into siRNA solution in RNase-free water in polymer-to-siRNA (N/P) ratios of 0.125, 0.25, 0.5, 0.75, 1, and 1.25 and incubated for 30 min at 37 °C to obtain siRNA polyplexes. Average particle size and zeta-potential measurements were estimated using Zetasizer Nano ZS (Malvern, UK). siRNA binding to PEI and displacement by anion competition was assessed by agarose gel electrophoresis as previously described (Alshamsan et al., 2009). Band intensity was analyzed using ImageJ software available from the National Institutes of Health at https://imagej.nih.gov/ij/.

3.2. Cellular uptake study

In 37 °C/5% CO_2 incubator, B16.F10 cells were grown and propagated in DMEM media supplemented with 2 mM L-glutamine, gentamicin, and 5% FBS. Then, cells were transferred to 6-well plate and incubated with 100 nM siRNA-polyplexes for designated time points after 50% confluence was reached. To assess cellular uptake by confocal laser scanning microscope (CLSM), B16.F10 cells were washed 3 times with PBS and immediately fixed with paraformaldehyde-PBS solution (2%) for 10 min. Dextran-Texas Red was added for 2 h at 37 °C to stain cytoskeleton. For flow cytometry (FCM) study, 5×10^4 cells were harvested at endpoint and washed 3 times with PBS and suspended in FCM buffer (5% FBS in PBS) and analyzed for percentage of positive cells by BD Accuri™ C6 Plus (BD Biosciences, Franklin Lakes, NJ).

3.3. STAT3 knockdown

Polyplexes of STAT3-targeting siRNA were prepared to give siRNA concentration of 200 nM that was serially diluted to the intended concentrations (200, 100, 50, 25, 12.5 and 6.25 nM). Thereafter, 1×10^5 B16 melanoma cells were incubated with siRNA polyplexes in 24-well plate for 24 h at 37 °C.

3.4. ELISA estimation of VEGF

Tumor supernatants were collected at 24 h point by gentle aspiration from cell culture flask and transferred to centrifuge tubes. To eliminate any floating cells, aspirated liquid was centrifuged at 10,000g for 5 min. Thereafter, supernatants were transferred to new centrifuge tubes. VEGF levels were determined by ELISA kit according to manufacturer's instruction.

3.5. Western blot analysis of p-STAT3

After 24 h, B16.F10 cells harvested by trypsin/EDTA and washed twice with ice-cold PBS and transferred to Eppendorf tubes imbedded in ice bucket. Cells were, then, lysed using lysis buffer containing 2 mM Na_3VO_4, 30 mM HEPES (pH 7.5), 2 mM EGTA, 2% NP-40,

0.5 mM dithiothreitol (DTT), and 1:100 protease/phosphatase inhibitor cocktail. Cell lysates were centrifuged for 20 sec at 16,000g. Thereafter, NaCl was added to samples to final concentration of 420 mM, cell lysates were centrifuged for 20 min at 16,000g. Supernatant was then transferred to new Eppendorf tubes, where and pellets were discarded and protein extract was determined using Micro BCA™ Protein Assay Kit. Thereafter, equal amounts of protein (20 µg) were mixed with equal volumes of loading buffer (0.5 M Tris-HCl pH 6.8, 20% glycerol, 10% SDS, 1.5% bromophenol blue, 5% 2-mercaptoethanol). Then, samples were dipped in boiling water for 5 min and then loaded on 10% SDS-PAGE gel. Electrophoresis was then conducted in Tris-Glycine SDS Running Buffer for 90 min. Proteins were then transferred into activated PVDF membrane using Bolt® Transfer Buffer containing methanol at 140 V for 2 h. Thereafter, the membrane was incubated overnight at 4 °C with Blocker BSA solution containing 0.1% (v/v) TWEEN® 20 that was also used to thoroughly wash membranes, where they are probed with antiphosphotyrosine (Y^{705}) STAT3 mAb (1:500) for 2 h. The membrane was then washed 5 times under gentle shaking. Then, goat antimouse polyclonal Ab (1:50,000) was added to the membranes in blocking buffer and kept at room temperature for 90 min under gentle shaking. Thereafter, the membrane was further 5 times before development using Amersham ECL Prime Western Blotting Detection Reagent kit. The membranes were then stripped, washed, blocked, and probed with anti-actin Ab (I-19) (1:1000) dilution and developed as previously described.

3.6. Cell viability assay

B16.F10 cells were grown in flat-bottomed 96-well microplates. After designated treatment, 100 µL MTT/culture media solution (500 µg/mL) was added in each well. After 3 h, formazan crystals were formed and were dissolved by adding 200 µL DMSO. Microplate reader was used to measure optical density at 550 nm and cell viability was calculated as percentage relevant to untreated control.

3.7. Data analysis

Statistical analysis was performed using SPSS for Windows, Version 16.0. Data were analyzed for statistical significance at $p < 0.05$. Where indicated, data represent average of 3 replicates with ±standard error.

4. Results

4.1. siRNA polyplexes characterization

Increment in the formulation zeta potential to N/P ratio was proportional until plateaued at N/P of 1 (Fig. 1a). Similarly, siRNA

association % in the polyplexes was proportional to the N/P ratio reaching toward plateau after N/P of 0.75 (Fig. 1b). At such N/P ratio, polyplexes showed hydrodynamic diameter range of 110 – 270 nm with average diameter of 172 nm (Fig. 1c). Moreover, the associated siRNA was shown to be releasable by anionic competition using heparin (Fig. 1d).

4.2. Cellular uptake of PEI- p-STAT3-siRNA

Uptake of siRNA polyplexes (PEI- p-STAT3-siRNA) by B16.F10 cells was assessed using CLSM and FCM. As shown in Fig. 2a, cell uptake started as early as 10 min following incubation with siRNA polyplexes. After 30 min of incubation, amount of internalized siRNA polyplexes were remarkably increased. Consistently, efficient cellular uptake was evident by FCM (Fig. 2b).
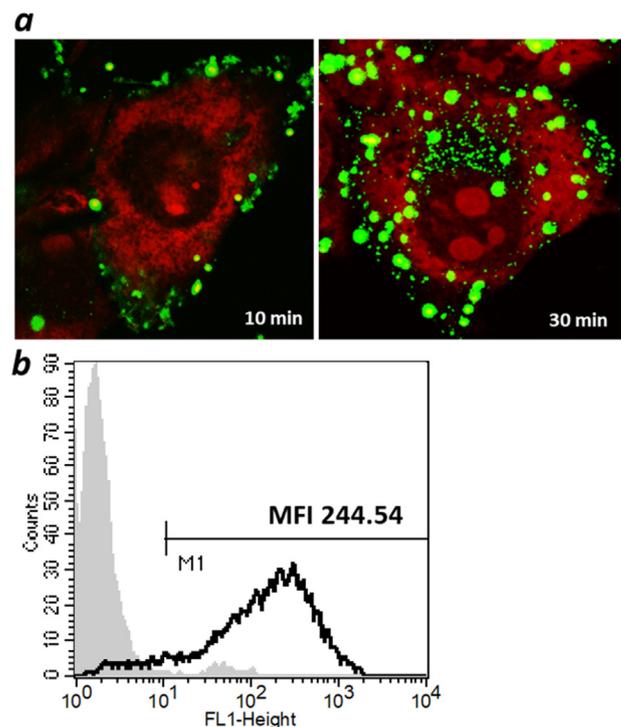

Fig. 2. FITC tagged PEI NPs were added to the B16.F10 melanoma cell cultures to investigate the uptake of the NPs. (a) Fluorescent micrograph revealed a significant uptake of PEI NPs after 30 min of addition. (b) Flowcytometry analysis confirmed the uptake of FITC tagged PEI NPs into B16.F10 melanoma cells.
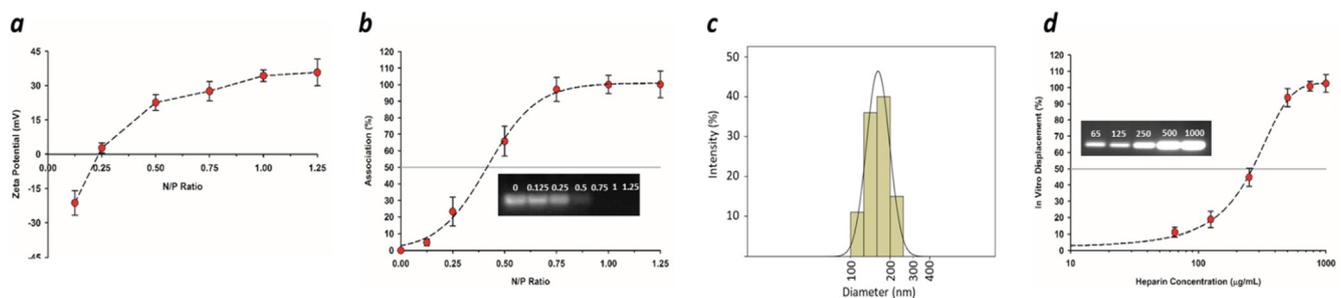

Fig. 1. siRNA polyplexes made by addition of PEI solution into siRNA solution in RNAse free water in different polymer to siRNA (N/P) ratios ranging from 0.125 to 1.25. The polyplexes were characterized by measuring average particle size and zeta-potential using Zetasizer Nano ZS (Malvern, UK). siRNA binding to PEI and dissociation was evaluated by agarose gel electrophoresis. (a) Increase in Zeta-potential of the particles remained proportional until N/P ratio reached 1.0. (b). Association % of siRNA with PEI increased upto an N/P ratio 0f 0.75. (c) Particle hydrodynamic diameter ranged from 110 to 270 nm with average diameter of 172 nm. (d) Anionic competition test using heparin exhibit dissociation of siRNA increased with increasing heparin concentration.
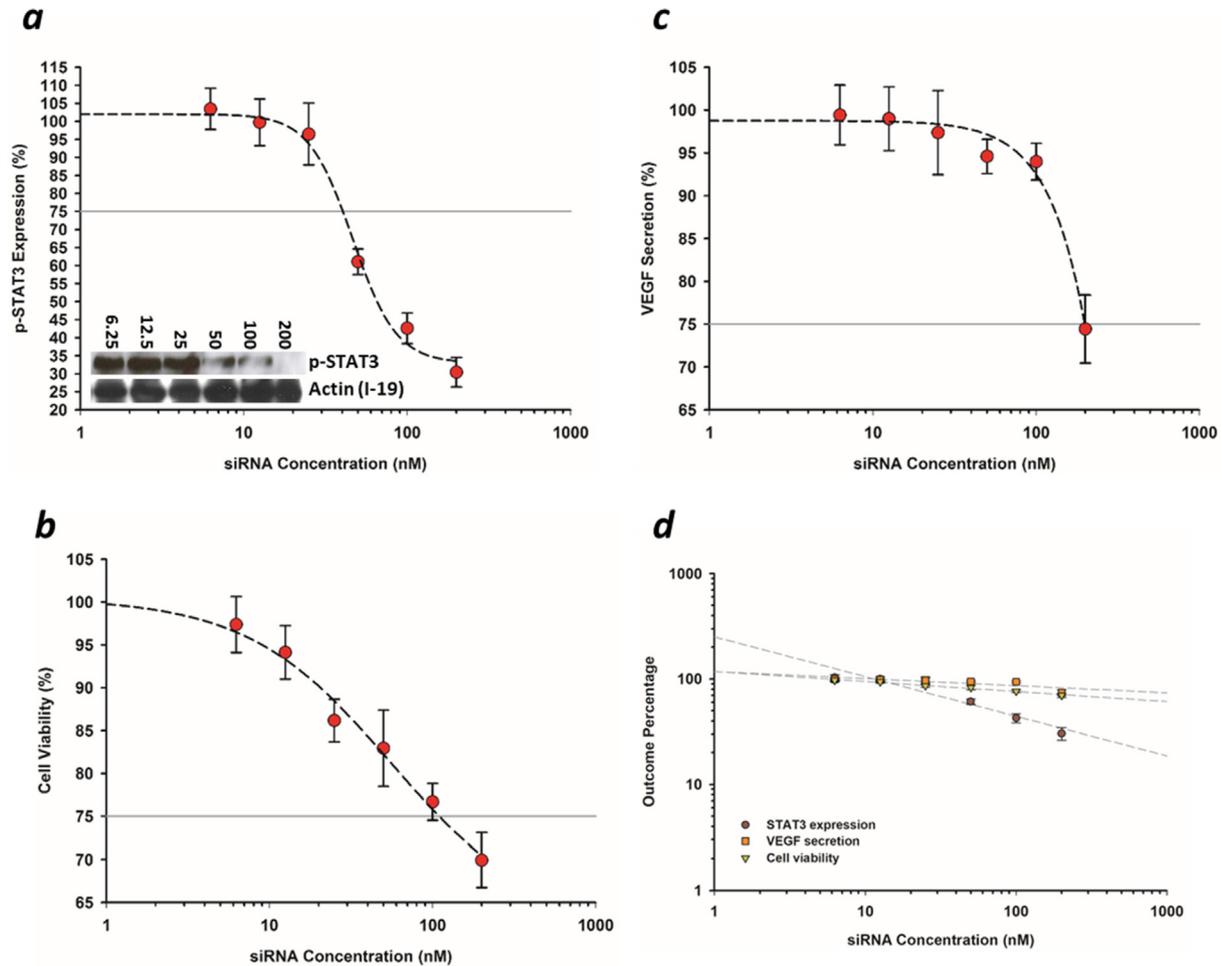
Fig. 3. (a) Western blot analysis reveal a concentration dependent knockdown of p-STAT3 in B16.F10 melanoma cells by PEI-p-STAT3-siRNA. (b) VEGF expression levels were not found to be correlated with that of p-STAT3 after addition of PEI-p-STAT3-siRNA. ELISA of VEGF indicate that the highest concentration of the STAT3-siRNA is needed to induce a significant downregulation of VEGF. (c) STAT3-siRNA induced cell death in B16.F10 melanoma cells was found to be concentration dependent. (d) Statistical analysis of the data found that the cell death is correlated more with VEGF levels than that of p-STAT3 after STAT3-siRNA administration.

4.3. siRNA interference outcomes

Molecular evidence of siRNA interference was evaluated by the expression of phosphorylated STAT3 (p-STAT3). As shown in Fig. 3a, p-STAT3 expression was inhibited upon siRNA incubation in a dose-dependent fashion. Significant reduction in p-STAT3 level was shown beyond 25 nM siRNA concentration and IC_{25} was reached around 40 nM. Concomitantly, dose-dependent inhibition of VEGF secretion was recorded, where IC_{25} was reached with siRNA concentration of 195 nM (Fig. 3b). Consistently, B16.F10 viability was reduced following dose-dependent siRNA administration reaching IC_{25} at 109 nM (Fig. 3c). To understand the correlation of the three outcomes of siRNA interference, the inhibition curves were plotted against siRNA concentration (Fig. 3d). Regression equation of all curved indicated high coefficient of determination (R^2) as shown in Table 1.

Table 1
Summary of Linear Regression analysis and R^2 values from different experiments including Western blot analysis of STAT3 expression, ELISA of VEGF protein and cell viability assay.

Outcome	Equation	R^2
STAT3 expression	y = −0.3952x + 98.479	0.8502
VEGF inhibition	y = −0.1203x + 100.87	0.9304
Cell viability	y = −0.1417x + 94.715	0.8428

5. Discussion

VEGF, which induces angiogenesis in developing fetuses and during wound healing in adults, when goes aberrant plays a significant role in tumor growth and survival (Verheul and Pinedo, 2000; Hicklin and Ellis, 2005). VEGF expression is regulated by p-STAT3, a transcription factor regulating several other genes' expression as well. For years, VEGF has been a subject of numerous cancer-associated studies and has been seen as a potential target for cancer therapy (Shinkaruk et al., 2003; Pradeep et al., 2005), so are the associated genes and proteins (Masciocchi et al., 2011; Santoni et al., 2015; Kim et al., 2016). p-STAT3 remains upstream to the VEGF and regulates its expression in response to various endogenous stimuli. Abnormally activated p-STAT3 has profound effects on tumor growth not only via escaping antitumor immune responses but also through tumor survival by pro-angiogenic effects of overexpressed VEGF (Chen and Han, 2008; Yu et al., 2009). Unregulated activation of STAT3 in cancer cells plays a significant role in bypassing apoptosis via suppressing transcription of proapoptotic genes (Timofeeva et al., 2013). Several strategies have been implemented in the past to inhibit STAT3 at protein or gene level. These strategies include STAT3 SH2 domain inhibition, upstream tyrosine kinase (JAK, Src) inhibition, DNA-binding domain inhibition and oligonucleotides (Fagard et al., 2013; Wong et al., 2017). In the past decade inhibition of STAT3 expres-

sion by small interfering RNA (siRNA) emerged as a promising strategy in anticancer therapy (Gao et al., 2005; Liu et al., 2010).

The present investigation aimed at PEI assisted delivery of p-STAT3-siRNA and its downstream effects on B16.F10 melanoma cells in-vitro. Acid-modified-polyethylenimine significantly enhanced uptake of p-STAT3-siRNA by B16.F10 melanoma cells. Reports published elsewhere also supported the role of acid-modified-polyethylenimine in assisting and enhancing delivery of similar oligonucleotides into the biological system (Guo et al., 2014; Borgheti-Cardoso et al., 2015; Ku et al., 2015). This enhancement is crucial in not only in absorption but also in reaching target, dose reduction and improving antitumor activities of p-STAT3-siRNA. Assembly of PEI- p-STAT3-siRNA has better advantages over unassisted delivery of the siRNA. Several research reports from different laboratories suggested nanocarrier assisted delivery of STAT3-siRNA has profound effects against tumorigenesis (Jia et al., 2012; Falamarzian et al., 2014; Herrmann et al., 2014) and induce antitumor immune responses (Luo, et al., 2015). The assembly as a nanoformulation has PEI-p-STAT3-siRNA complexes of a size around 100 nm and data from fluorescence and confocal microscopy reveal the significant uptake of these assemblies into B16.F10 melanoma cells. These findings were also confirmed by flowcytometric analysis. Increased intracellular uptake of p-STAT3-siRNA certainly increased the knockdown effect on p-STAT3, an effect that reaches downstream to VEGF and associated functions.

p-STAT3-siRNA administration at six different concentrations exhibited a concentration-dependent silencing of the p-STAT3. In the identical experimental setup, these effects were found to be less profound on VEGF expression by all the different concentration levels of PEI-p-STAT3-siRNA, except the highest one. The absence of dose-response relation between PEI-p-STAT3-siRNA and VEGF expression ascertain that STAT3 inhibition and VEGF downregulation are not proportionally correlated and VEGF downregulation remains a secondary outcome of STAT3 silencing. Only higher concentrations of PEI-p-STAT3-siRNA significantly downregulated the expression of VEGF via knockdown of p-STAT3. Experiments with lower concentrations of PEI-p-STAT3-siRNA could not find any significant down regulation of VEGF. Cell viability investigation revealed decreasing cell survival with increasing concentration of PEI-p-STAT3-siRNA and a correlation with both p-STAT3 knockdown and downregulation of VEGF. However, the cell death was found to be correlated with VEGF expression rather than that of p-STAT3 knockdown itself. It may be suggested that VEGF expression levels are playing a crucial role in cancer cell death induced by addition of PEI-p-STAT3-siRNA. Normally, VEGF remains involved in angiogenesis and cell survival (Byrne et al., 2005), though the cell protection role appears to be prevalent regardless of the cell type, cells' health status or ambient environment. For instance, VEGF is reported to play a significant role in cell survival by inhibiting apoptotic cell death against chemotherapeutic drugs in hematopoietic cells (Katoh et al., 1998) and high glucose in endothelial cells (Yang et al., 2008). Other than its role in normal conditions, it has also been suggested to act as a survival factor for tumor cells and protect them from apoptosis (Pidgeon et al., 2001; Harmey and Bouchier-Hayes, 2002). The outcome of the present investigation emphasizes the significant role of VEGF downregulation and reduced survival of B16.F10 melanoma cells by the p-STAT3 knockdown.

Though these findings in B16.F10 melanoma cells does not rule out any significant involvement of p-STAT3 regulated immune responses associated with tumorigenesis in in-vivo conditions. During in-vivo investigation, PEI-p-STAT3-siRNA administration significantly suppressed orthotopic B16.F10 melanoma in syngeneic C57BL/6 mice (Data not shown). In our previous report, it has been demonstrated that STAT3-siRNA intervention induced around fivefold infiltration of CD3^{+} cells and fourfold of dendritic cells into tumors in BALB/c and C57BL/6 following STAT3 knockdown. High levels of CD4^{+}, CD8^{+}, and NKT cells were also observed in the tumors along with CD3^{+} cells (Alshamsan et al., 2011). It may be suggested that VEGF downregulation along with induction of antitumor immunity is central to the tumor suppressive mechanism of STAT3-siRNA induced STAT3 knockdown. In tumor cells, signaling downstream to VEGF is mediated by VEGF receptor tyrosine kinases (RTKs) and neuropilins (NRPs) (Goel and Mercurio, 2013). It remains a subject of further investigation what effects PEI-p-STAT3-siRNA has on VEGF-RTKs and NRPs in-vitro and in-vivo in association with tumorigenesis.

6. Conclusion

On the basis of outcomes, the present investigation highlights that the assembly of STAT3-siRNA with PEI NPs enhances its cellular uptake and contributes to improve its antitumor effectiveness. VEGF downregulation has been found to play significant role in B16.F10 melanoma cell death after STAT3 knockdown and its role appear to be more predictive than STAT3 levels in this case. Moreover, high concentrations of PEI-p-STAT3-siRNA are needed to downregulate VEGF expression via STAT3 knockdown. However, STAT3-siRNA silenced p-STAT3 in a concentration dependent manner; the effects are not found to be proportionally correlated with VEGF downregulation. Further investigation is needed to investigate STAT3-siRNA effects downstream to VEGF.

7. Disclosure of interest

The author reports no conflict of interest.

References

Alshamsan, A., Haddadi, A., Incani, V., Samuel, J., Lavasanifar, A., Uludag, H., 2009. Formulation and delivery of siRNA by oleic acid and stearic acid modified polyethylenimine. Mol Pharm. 6 (1), 121–133.

Alshamsan, A., Hamdy, S., Samuel, J., El-Kadi, A.O., Lavasanifar, A., Uludag, H., 2010. The induction of tumor apoptosis in B16 melanoma following STAT3 siRNA delivery with a lipid-substituted polyethylenimine. Biomaterials. 31 (6), 1420–1428.

Alshamsan, A., Hamdy, S., Haddadi, A., Samuel, J., El-Kadi, A.O., Uludag, H., Lavasanifar, A., 2011. STAT3 Knockdown in B16 Melanoma by siRNA Lipopolyplexes Induces Bystander Immune Response In Vitro and In Vivo. Transl Oncol. 4 (3), 178–188.

Azimi, A., Majidinia, M., Shafiei-Irannejad, V., Jahanban-Esfahlan, R., Ahmadi, Y., Karimian, A., Mir, S.M., Karami, H., Yousefi, B., 2017. Suppression of p53R2 gene expression with specific siRNA sensitizes HepG2 cells to doxorubicin. Gene.

Borgheti-Cardoso, L.N., Depieri, L.V., Kooijmans, S.A., Diniz, H., Calzzani, R.A., Vicentini, F.T., van der Meel, R., Fantini, M.C., Iyomasa, M.M., Schiffelers, R.M., et al., 2015. An in situ gelling liquid crystalline system based on monoglycerides and polyethylenimine for local delivery of siRNAs. Eur. J. Pharm. Sci. 74, 103–117.

Byrne, A.M., Bouchier-Hayes, D.J., Harmey, J.H., 2005. Angiogenic and cell survival functions of vascular endothelial growth factor (VEGF). J. Cell Mol. Med. 9 (4), 777–794.

Carmeliet, P., 2005. VEGF as a key mediator of angiogenesis in cancer. Oncology 69 (Suppl 3), 4–10.

Chen, Z., Han, Z.C., 2008. STAT3: a critical transcription activator in angiogenesis. Med. Res. Rev. 28 (2), 185–200.

De Rosa, G., Salzano, G., 2015. PLGA microspheres encapsulating siRNA. Methods Mol. Biol. 1218, 43–51.

Dutta, P., Sabri, N., Li, J., Li, W.X., 2014. Role of STAT3 in lung cancer. JAKSTAT 3 (4), e999503.

Fagard, R., Metelev, V., Souissi, I., Baran-Marszak, F., 2013. STAT3 inhibitors for cancer therapy: Have all roads been explored? JAKSTAT 2 (1), e22882.

Falamarzian, A., Aliabadi, H.M., Molavi, O., Seubert, J.M., Lai, R., Uludag, H., Lavasanifar, A., 2014. Effective down-regulation of signal transducer and activator of transcription 3 (STAT3) by polyplexes of siRNA and lipid-substituted polyethyleneimine for sensitization of breast tumor cells to conventional chemotherapy. J. Biomed. Mater Res. A. 102 (9), 3216–3228.

Furtek, S.L., Backos, D.S., Matheson, C.J., Reigan, P., 2016. Strategies and approaches of targeting STAT3 for cancer treatment. ACS Chem. Biol. 11 (2), 308–318.

Gao, L.F., Xu, D.Q., Wen, L.J., Zhang, X.Y., Shao, Y.T., Zhao, X.J., 2005. Inhibition of STAT3 expression by siRNA suppresses growth and induces apoptosis in laryngeal cancer cells. Acta Pharmacol. Sin. 26 (3), 377–383.

Goel, H.L., Mercurio, A.M., 2013. VEGF targets the tumour cell. Nat. Rev. Cancer 13 (12), 871–882.

Guo, Z., Li, Y., Fu, Y., Guo, T., Li, X., Yang, S., Xie, J., 2014. Enhanced antisense oligonucleotide delivery using cationic liposomes incorporating fatty acid-modified polyethylenimine. Curr. Pharm. Biotechnol. 15 (9), 800–805.

Hansen, W., Hutzler, M., Abel, S., Alter, C., Stockmann, C., Kliche, S., Albert, J., Sparwasser, T., Sakaguchi, S., Westendorf, A.M., et al., 2012. Neuropilin 1 deficiency on CD4+Foxp3+ regulatory T cells impairs mouse melanoma growth. J. Exp. Med. 209 (11), 2001–2016.

Harmey, J.H., Bouchier-Hayes, D., 2002. Vascular endothelial growth factor (VEGF), a survival factor for tumour cells: implications for anti-angiogenic therapy. Bioessays. 24 (3), 280–283.

Herrmann, A., Priceman, S.J., Swiderski, P., Kujawski, M., Xin, H., Cherryholmes, G.A., Zhang, W., Zhang, C., Lahtz, C., Kowolik, C., et al., 2014. CTLA4 aptamer delivers STAT3 siRNA to tumor-associated and malignant T cells. J. Clin. Invest. 124 (7), 2977–2987.

Hicklin, D.J., Ellis, L.M., 2005. Role of the vascular endothelial growth factor pathway in tumor growth and angiogenesis. J. Clin. Oncol. 23 (5), 1011–1027.

Huang, W.Y., Chen, D.H., Ning, L., Wang, L.W., 2017. siRNA mediated silencing of NIN1/RPN12 binding protein 1 homolog inhibits proliferation and growth of breast cancer cells. Asian Pac. J. Cancer Prev. 18 (10), 2891.

Jia, H., Li, Y., Zhao, T., Li, X., Hu, J., Yin, D., Guo, B., Kopecko, D.J., Zhao, X., Zhang, L., et al., 2012. Antitumor effects of Stat3-siRNA and endostatin combined therapies, delivered by attenuated Salmonella, on orthotopically implanted hepatocarcinoma. Cancer Immunol. Immunother. 61 (11), 1977–1987.

Johnson, D.E., O'Keefe, R.A., Grandis, J.R., 2018. Targeting the IL-6/JAK/STAT3 signalling axis in cancer. Nat. Rev. Clin. Oncol. 15 (4), 234–248.

Katoh, O., Takahashi, T., Oguri, T., Kuramoto, K., Mihara, K., Kobayashi, M., Hirata, S., Watanabe, H., 1998. Vascular endothelial growth factor inhibits apoptotic death in hematopoietic cells after exposure to chemotherapeutic drugs by inducing MCL1 acting as an antiapoptotic factor. Cancer Res. 58 (23), 5565–5569.

Kim, B.H., Yi, E.H., Ye, S.K., 2016. Signal transducer and activator of transcription 3 as a therapeutic target for cancer and the tumor microenvironment. Arch. Pharm. Res. 39 (8), 1085–1099.

Krivitsky, A., Polyak, D., Scomparin, A., Eliyahu, S., Ofek, P., Tiram, G., Kalinski, H., Avkin-Nachum, S., Gracia, N.F., Albertazzi, L., et al., 2017. Amphiphilic poly (alpha)glutamate polymeric micelles for systemic administration of siRNA to tumors. Nanomedicine.

Ku, S.H., Hong, J., Moon, H.H., Jeong, J.H., Mok, H., Park, S., Choi, D., Kim, S.H., 2015. Deoxycholic acid-modified polyethylenimine based nanocarriers for RAGE siRNA therapy in acute myocardial infarction. Arch. Pharm. Res. 38 (7), 1317–1324.

Kut, C., Mac Gabhann, F., Popel, A.S., 2007. Where is VEGF in the body? A meta-analysis of VEGF distribution in cancer. Br. J. Cancer 97 (7), 978–985.

Liu, Y., Li, P.K., Li, C., Lin, J., 2010. Inhibition of STAT3 signaling blocks the anti-apoptotic activity of IL-6 in human liver cancer cells. J. Biol. Chem. 285 (35), 27429–27439.

Luo, Z., Wang, C., Yi, H., Li, P., Pan, H., Liu, L., Cai, L., Ma, Y., 2015. Nanovaccine loaded with poly I: C and STAT3 siRNA robustly elicits anti-tumor immune responses through modulating tumor-associated dendritic cells in vivo. Biomaterials 38, 50–60.

Masciocchi, D., Gelain, A., Villa, S., Meneghetti, F., Barlocco, D., 2011. Signal transducer and activator of transcription 3 (STAT3): a promising target for anticancer therapy. Future Med. Chem. 3 (5), 567–597.

Pidgeon, G.P., Barr, M.P., Harmey, J.H., Foley, D.A., Bouchier-Hayes, D.J., 2001. Vascular endothelial growth factor (VEGF) upregulates BCL-2 and inhibits apoptosis in human and murine mammary adenocarcinoma cells. Br. J. Cancer 85 (2), 273–278.

Pradeep, C.R., Sunila, E.S., Kuttan, G., 2005. Expression of vascular endothelial growth factor (VEGF) and VEGF receptors in tumor angiogenesis and malignancies. Integr. Cancer Ther. 4 (4), 315–321.

Ruvinov, E., Kryukov, O., Forti, E., Korin, E., Goldstein, M., Cohen, S., 2015. Calcium-siRNA nanocomplexes: what reversibility is all about. J. Controll. Release: Off. J. Controll. Release Soc. 203, 150–160.

Santoni, M., Massari, F., Del Re, M., Ciccarese, C., Piva, F., Principato, G., Montironi, R., Santini, D., Danesi, R., Tortora, G., et al., 2015. Investigational therapies targeting signal transducer and activator of transcription 3 for the treatment of cancer. Expert Opin. Investig. Drugs. 24 (6), 809–824.

Shinkaruk, S., Bayle, M., Lain, G., Deleris, G., 2003. Vascular endothelial cell growth factor (VEGF), an emerging target for cancer chemotherapy. Curr. Med. Chem. Anticancer Agents 3 (2), 95–117.

Timofeeva, O.A., Tarasova, N.I., Zhang, X., Chasovskikh, S., Cheema, A.K., Wang, H., Brown, M.L., Dritschilo, A., 2013. STAT3 suppresses transcription of proapoptotic genes in cancer cells with the involvement of its N-terminal domain. Proc. Natl. Acad. Sci. USA 110 (4), 1267–1272.

Verheul, H.M., Pinedo, H.M., 2000. The role of vascular endothelial growth factor (VEGF) in tumor angiogenesis and early clinical development of VEGF-receptor kinase inhibitors. Clin. Breast Cancer 1 (Suppl 1), S80–84.

Wei, D., Le, X., Zheng, L., Wang, L., Frey, J.A., Gao, A.C., Peng, Z., Huang, S., Xiong, H.Q., Abbruzzese, J.L., et al., 2003. Stat3 activation regulates the expression of vascular endothelial growth factor and human pancreatic cancer angiogenesis and metastasis. Oncogene. 22 (3), 319–329.

Wong, A.L.A., Hirpara, J.L., Pervaiz, S., Eu, J.Q., Sethi, G., Goh, B.C., 2017. Do STAT3 inhibitors have potential in the future for cancer therapy? Expert Opin. Investig. Drugs. 26 (8), 883–887.

Yang, Z., Mo, X., Gong, Q., Pan, Q., Yang, X., Cai, W., Li, C., Ma, J.X., He, Y., Gao, G., 2008. Critical effect of VEGF in the process of endothelial cell apoptosis induced by high glucose. Apoptosis. 13 (11), 1331–1343.

Yu, H., Pardoll, D., Jove, R., 2009. STATs in cancer inflammation and immunity: a leading role for STAT3. Nat. Rev. Cancer 9 (11), 798–809.

Yu, H., Lee, H., Herrmann, A., Buettner, R., Jove, R., 2014. Revisiting STAT3 signalling in cancer: new and unexpected biological functions. Nat. Rev. Cancer 14 (11), 736–746.

Yue, P., Turkson, J., 2009. Targeting STAT3 in cancer: how successful are we? Expert Opin. Investig. Drugs. 18 (1), 45–56.